J. Mex. Chem. Soc. **2025**, *69*(1)
Special Issue

ISSN-e 2594-0317

Advancements in Understanding Nucleation and Growth Phenomena Of Electrochemical Phase Formation Processes: Contributions from UAM Research

Manuel Eduardo Palomar-Pardavé

Universidad Autónoma Metropolitana-Azcapotzalco, Departamento de Materiales, Av. San Pablo 180, Col. Reynosa-Tamaulipas, C.P. 02200, CDMX, México.

***Corresponding author:** Manuel Eduardo Palomar-Pardavé, email: mepp@azc.uam.mx

Received May 22nd, 2024; Accepted August 6th, 2024.

DOI: http://dx.doi.org/10.29356/jmcs.v69i1.2287

Abstract. This work entails a review of the research conducted at "Universidad Autónoma Metropolitana", UAM, on the nucleation and growth phenomena involved during the electrochemical phase formation processes (EPF). Specifically, these processes include metal electrodeposition, electrosynthesis of conductive polymers or synthetic metals, anodic film formation, and the electrochemical condensation of surfactant micelles. The primary contributions of these studies focus on developing chemical-physical theoretical models capable of determining the mechanism and kinetics of these EPF processes. This is achieved through the analysis of experimental potentiostatic current density transients recorded in both aqueous and deep eutectic solvents. Furthermore, the resulting modified electrodes are applied to various significant applications, such as green energy generation using direct alcohol fuel cells, the development of electrochemical sensors for neurotransmitters and other biologically important substances, and corrosion and environmental protection.
Keywords: Nucleation; growth; electrochemical phase formation; nanoparticles; deep eutectic solvents.

Resumen. Este trabajo revisa la investigación realizada en la Universidad Autónoma Metropolitana (UAM) sobre los fenómenos de nucleación y crecimiento involucrados en los procesos de formación electroquímica de fases (EPF). Específicamente, estos procesos incluyen la electrodeposición de metales, la electrosíntesis de polímeros conductores o metales sintéticos, la formación de películas anódicas y la condensación electroquímica de micelas de surfactantes. Las principales contribuciones de estos estudios se centran en el desarrollo de modelos teóricos fisicoquímicos capaces de determinar los mecanismos y la cinética de estos procesos EPF. Esto se logra a través del análisis de transitorios potenciostáticos de densidad de corriente experimentales registrados en disolventes acuosos y eutécticos profundos. Además, los electrodos modificados resultantes se utilizan en diversas aplicaciones significativas, como la generación de energía verde mediante celdas de combustible de alcoholes directos, el desarrollo de sensores electroquímicos para neurotransmisores y otras sustancias biológicamente importantes, así como la protección contra la corrosión y la protección ambiental.
Palabras clave: Nucleación; crecimiento; formaciones electroquímicas de fases; nanopartículas; disolventes eutécticos profundos.

J. Mex. Chem. Soc. **2025**, *69*(1)
Special Issue

ISSN-e 2594-0317

Introduction

After 50 years of chemistry at the Universidad Autónoma Metropolitana (UAM), many significant contributions to this central science have been achieved by its community. These results stem from the synergistic relationship between teaching and research, a core aspect promoted by UAM as part of its foundational functions. Particularly noteworthy are contributions in fundamental and applied electrochemistry involving electrochemical phase formation processes [1-79]. This work serves as a comprehensive review of some of these investigations, showcasing collaborative efforts among various UAM campuses (Azcapotzalco, Iztapalapa and Xochimilco) as well as with prominent national institutions (Instituto Politécnico Nacional and Instituto Mexicano del Petróleo) and international partners (Universidad Simón Bolivar, Caracas, Venezuela and Phenikaa University, Hanoi, Vietnam).

Electrochemical phase formation

Electrochemical Phase Formation (**EPF**) **[80-86]** refers to the processes through which different phases or states of matter are formed or transformed via electrochemical reactions. These processes involve nucleation, growth, and transformation of phases or materials at electrode surfaces under specific electrochemical conditions. **EPF** is essentially a phase transition reaction triggered by changes in the oxidation state of a substance. It is extensively studied in the realm of electrochemistry, where electrical energy drives chemical reactions.

Understanding **EPF** holds significant importance across various fields such as materials science and engineering, chemical engineering [13,14,17,22,24,27,37,39,47,53,56,66], battery technology [49,52,54,59, 66], corrosion prevention/protection [7,26,32], electroplating and nanoparticles modified electrodes [1-6,8-10,12,17,18,21,28,30,32,37-39-57,59-69], sensors [15,16,19,20,23,25,29,31,33-37,58,61], and environmental electrochemistry [5,11,15,49,52,54,59,66], among others. Here's an overview of key concepts related to understanding **EPF**:

Nucleation: Nucleation is the initial step in **EPF** where clusters of atoms, ions, or molecules come together to form stable nuclei on the surface of an electrode during an electrochemical reaction. These nuclei are the starting points from which further growth occurs. In electrochemistry, nucleation is often characterized by the formation of tiny crystallites or clusters of atoms or molecules that have different properties from the bulk material or solution. This process is influenced by factors such as supersaturation, surface energy, electrode potential, and electrolyte composition [82,83].

Growth: After nucleation, the nuclei grow by the addition of species from the electrolyte onto the nuclei. The growth process can lead to the formation of larger crystalline structures, thin films, coatings, or other types of deposits on the electrode surface, depending on the specific electrochemical conditions and materials involved. The growth kinetics depend on diffusion rates, deposition potential, surface roughness, and the nature of the deposited material. Together, nucleation and growth processes govern the overall phase formation and structure evolution in electrochemical systems, influencing properties such as morphology, crystallographic orientation, grain size, and surface roughness [82].

Transformation: **EPF** can involve phase transformations, where the deposited material undergoes changes in crystal structure, morphology, or chemical composition. These transformations can occur due to changes in electrochemical conditions, temperature, or applied potentials [83].

Experimental Techniques: Various experimental techniques are used to study **EPF**, including cyclic voltammetry, chronoamperometry, scanning electron microscopy (SEM), X-ray diffraction (XRD), atomic force microscopy (AFM), X-ray energy dispersion spectroscopy (EDX) and X-ray photoelectron spectroscopy (XPS). These techniques provide insights into nucleation rates, growth mechanisms, surface morphology, crystallographic orientation, and phase transformations and composition [1-86]. Furthermore, a combined potentiostatic-galvanostatic pulse method has been also reported to study **EPF** [81] however, its application by the community has been very limited.

Theoretical Models: Chemical-physical theoretical models, such as classical and atomistic nucleation theory [38,41,69,70], multiple two-dimensional (2D) [4,7, 8, 9,28,30,32,37,42,65], see Fig. 1**(a)**, and three-dimensional (3D) nucleation [1-8,10,12-14,17,18,21,22,24,26,30,32,38-57,59-69], see Fig. 1**(b)**, with lattice incorporation, Fig. 1**(a)**, or diffusion-controlled growth, Fig. 1**(b)**, models, and Monte Carlo simulations [3], are

J. Mex. Chem. Soc. **2025**, *69*(1)
Special Issue

ISSN-e 2594-0317

employed to understand and predict **EPF** kinetics, mechanisms, and thermodynamics. The electrochemical technique that has proven to be most useful for gaining a fundamental understanding of **EPF** is undoubtedly chronoamperometry where the current, *i*, or the current density, *j*, is measured as a function of time when a constant potential is imposed to the working electrode. The analysis of experimental *j-t* plots in the context of the various theoretical formalisms developed [3,4,12,81-86], see also Table 1.1 in [82], makes it possible to determine, among other things, the dimensionality of the deposit (2D, 3D), the limiting stage of the overall process (incorporation of atoms, diffusion), as well as the mechanisms and kinetics of the electrodeposition process (nucleation frequency, A, number density of active sites, N_0, bulk diffusion coefficients, D). For instance meanwhile copper underpotential deposition onto a single crystal [4,9,18,28,30] or polycrystal [28,30] bulk gold electrode or gold nanoparticles supported onto an ITO [37] or Si(111) [42] electrodes involves the formation of a 2D monolayer (the broken red-line in the *j-t* plot depicted Figure 1a, was obtaining as the ratio Q_{2D} / Q_{ML} where Q_{2D} is the experimental charge density obtained by integration of the *j-t* plot and Q_{ML} corresponds to the theoretical maximum charge density, at full coverage of a the depositing metal monolayer), the silver electrodeposition onto vitreous carbon [1-3,41], indium tin oxide [38], TiO_2 nanotubes anodically formed on Ti [63] electrodes occurs via 3D nucleation. The 2D-3D nucleation transition, see Figure 3d, has been demonstrated to occur during potentiostatic metal deposition with underpotential and overpotential deposition processes [4], and recently demonstrated to occur during the potentiostatic zinc electrodeposition from reline deep eutectic solvent [65] onto a vitreous carbon electrode. Often these metallic centers depicts electrocatalytic activity toward some compounds present in the electrolytic baths, provoking that side faradaic reaction occurring on the growing surfaces of a 3D nucleus electrodeposited onto a foreign substrate (for instances nitrate [5] or protons reduction onto 3D cobalt nuclei diffusion-controlled growth [12,39] form aqueous media or residual water reduction onto nickel [44,62], aluminum [48,57], iron [50], palladium [51,53,56], nickel-cobalt alloy [52,64,66], chromium [55,68], cobalt [59,67], gold [61], nanoparticles potentiostatically deposited onto glassy carbon from a deep eutectic solvent.

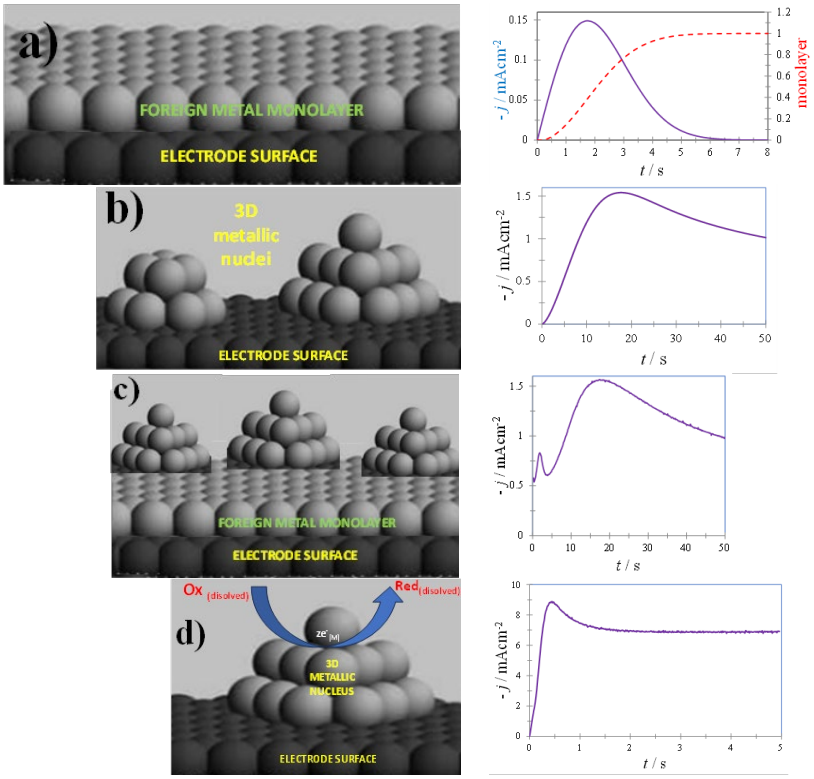

Fig. 1. Schemes, left, and its corresponding potentiostatic current density transient, right, of **(a)** a 2D monolayer of a metal onto a different nature substrate **(b)** 3D nuclei electrodeposited onto a foreign nature electrode **(c)** 2D-3D transition, growth mode called Stranski–Krastanov [65] and **(d)** a concomitant faradaic reaction occurring on the growing surfaces of a 3D nucleus electrodeposited onto a foreign substrate.

J. Mex. Chem. Soc. **2025**, *69*(1)
Special Issue

ISSN-e 2594-0317

Applications: The fundamental comprehension of **EPF** is essential for various applications, including electrodeposition of metals and alloys from aqueous (for instance silver [1-3,10,38,41], copper [4,9,18,28,30,37,42], cobalt [5,6,8,12,39], chromium [21], palladium [40], lead-base alloys [7] and from the recently developed deep eutectic solvents (silver [41, 54, 63], cobalt [43,45,59,67], nickel [44, 62], iron [46,50], palladium [47,51,53,56], aluminum [48, 57], chromium [55,68], gold [61,63], zinc [65], Mn-Zn Alloy [49], Ni–Co alloy [52,64,66], Pd-Co alloy [60]), synthesis of conducting polymers (electropolymerization of 5-Amino-1,10-phenthroline[13], pyrrole electropolymerization [14,15,17,22,24,27,29], β-cyclodextrin electropolymerization [25,33-36], fabrication of nanostructures, development of electrochemical sensors devices [15,16,19,20,23,25,29,31,33-37,58,61], corrosion protection [7,26,32], and energy storage/conversion systems like batteries and fuel cells [47,53,56,66].

By integrating experimental investigations with theoretical models, researchers can advance their understanding of **EPF** processes and harness them for innovative technological applications across different industries. Understanding nucleation and growth processes in electrochemical systems is crucial for several reasons:

1. Controlled Material Synthesis: Knowledge of nucleation and growth kinetics allows researchers and engineers to control the formation and growth of materials with desired properties. This control is essential for producing materials with specific characteristics such as size [37,44,47,50,51,53,55,56,60,61,63,68], shape [53,55,57,65], crystallographic orientation [45], and surface morphology [57].
2. Enhanced Performance: Optimizing nucleation and growth can lead to materials and coatings with improved performance in various applications. For example, in battery technology, controlling nucleation and growth can enhance electrode efficiency and cycle life. In corrosion protection, it can lead to more effective and durable coatings.
3. Tailored Properties: By understanding nucleation and growth, it becomes possible to tailor the properties of materials for specific purposes. This includes tuning electrical, mechanical, optical, and catalytic properties [47,53,56,66] to meet the requirements of different electrochemical devices and processes.
4. Efficiency and Cost-Effectiveness: Efficient nucleation and growth processes can lead to reduced energy consumption and improved resource utilization in electrochemical manufacturing processes. This can result in cost savings and environmental benefits.
5. Prevention of Undesirable Phenomena: Understanding nucleation and growth helps in avoiding undesirable phenomena such as dendritic growth, which can cause short circuits in batteries or reduce the quality of electrodeposited coatings. By controlling these processes, it becomes possible to mitigate such issues.
6. Advanced Device Design: Insights into nucleation and growth enable the design of advanced electrochemical devices with enhanced functionalities. This includes the development of novel electrode materials, coatings with tailored properties, and innovative nanostructures for sensing, energy storage, and conversion applications.
7. Electrodeposition and Coating Formation: Nucleation: Controls the initiation of electrodeposition, influencing the density and size distribution of nuclei formed on the substrate surface. Growth: Dictates the thickness, uniformity, adhesion, and microstructure of electrodeposited coatings or layers, impacting properties such as corrosion resistance, wear resistance, and electrical conductivity. Applications: Important in industries such as automotive (for coatings on components), electronics (for circuit board fabrication), and aerospace (for protective coatings on aircraft parts).
8. Battery Technology: Nucleation: Affects the formation of electrode materials during battery cycling, influencing battery capacity, cycling stability, and charge/discharge kinetics. Growth: Determines the morphology and stability of electrode materials, impacting factors like ion diffusion, electrode surface area, and mechanical integrity. Applications: Crucial for the development of high-performance lithium-ion batteries, solid-state batteries, and next-generation energy storage technologies.
9. Corrosion Protection: Nucleation: Controls the formation of corrosion-inhibiting films or coatings on metal surfaces, influencing their adhesion, thickness, and barrier properties. Growth: Determines the long-term stability and effectiveness of corrosion protection coatings, affecting factors like porosity, defect density, and chemical resistance. Applications: Essential in infrastructure (bridges, pipelines), marine environments (ships, offshore structures), and automotive (vehicle chassis, engine components) for preventing corrosion-related damage.

J. Mex. Chem. Soc. **2025**, *69*(1)
Special Issue

ISSN-e 2594-0317

10. Sensor Technology: Nucleation: Impacts the formation of sensing layers or materials in electrochemical sensors, affecting sensitivity, selectivity, and response time. Growth: Influences the morphology and surface area of sensing materials, optimizing interactions with target analytes and enhancing sensor performance. Applications: Used in environmental monitoring (air quality sensors, water quality sensors), healthcare (biosensors, medical diagnostics), and industrial process control (gas sensors, chemical sensors).

11. Nanomaterial Synthesis: Nucleation: Governs the formation of nanoparticles or nanostructures with controlled size, shape, and crystallinity, affecting their electronic, optical, and catalytic properties. Growth: Determines the growth kinetics and stability of nanomaterials, influencing properties such as surface plasmon resonance, quantum confinement effects, and catalytic activity. Applications: Utilized in nanoelectronics (quantum dots, nanowires), catalysis (nanoparticle catalysts), and materials science (nanocomposites, nanofilms) for advanced functionalities and performance enhancements.

In each of these areas, understanding and optimizing nucleation and growth processes are essential for achieving desired material properties, enhancing performance characteristics, and advancing technological capabilities in electrochemical applications.

The electrodeposition of some electrocatalytic metal nuclei (i.e. cobalt [5,12,21,39,45,52], iron [50], nickel [44,52,62], chromium [55,68], aluminum [48,57], palladium [51,53,56]), gold [61] from aqueous media [5,12,21,39] or deep eutectic solvents [44,45,48,50-53,55,56,61], is generally accompanied by a side faradaic reaction namely: nitrates [5,21] protons [12,21,39] or water reduction [44,45,48,50-53,55,56,61], see R1, which is a reaction capable of diminishing the cathodic efficiency, inducing brittleness of the metallic deposit due to hydrogen embrittlement, in some cases or modify the chemical composition of the electrodepositing nuclei [44,48,51,53,56,57].

$$2H_2O_{DES} + 2e^-{}_{(Metal)} \underset{\longleftarrow}{\longrightarrow} H_{2_{(g)}} + 2OH_{DES}{}^- \qquad \text{(R1)}$$

An example of analyzing an EPF process using a theoretical model developed at UAM

In the case of palladium nanoparticles (PdNPs) electrodeposition onto a glassy carbon electrode (GCE) from Pd(II) ions dissolved in deep eutectic solvents (DES), such as ethaline [47] or reline [51,53,56], the resulting modified electrode (GCE/PdNPs) demonstrates outstanding performance in the formic acid oxidation reaction (FAOR) [47,56] and methanol oxidation reactions (MOR) [56]. Both FAOR and MOR are crucial for the green generation of energy in direct alcohol fuel cell devices. The analysis of the experimental *j-t* plots was conducted using the formalism proposed by Palomar-Pardavé *et al***.** [12], see Eqn. (1). This formalism considers that two contributions to the total current, (j_{total}) may occur simultaneously: j_{3D}, due to 3D nucleation and diffusion-controlled growth of metal aggregates (in this case Pd), and j_{WR}, the individual contribution of a faradaic process (in this case the residual water reduction on the surface of the growing Pd nuclei).

$$j_{total}(t) = j_{3D}(t) + j_{WR}(t) \qquad (1)$$

with

$$j_{3D}(t) = P_1 t^{-1/2} \frac{\Phi}{\varphi} \theta(t) \qquad (2)$$

$$j_{WR}(t) = P_3 \theta(t) \qquad (3)$$

where

J. Mex. Chem. Soc. **2025**, *69*(1)
Special Issue

ISSN-e 2594-0317

$$\theta(t) = (1 - \exp(-P_2 t\varphi(t))) \tag{4}$$

$$\varphi(t) = 1 - \frac{1 - exp(-At)}{\mathrm{A}t} \tag{5}$$

$$\Phi(t) = 1 - \frac{exp(-At)}{(\mathrm{A}t)^{\frac{1}{2}}} \int_0^{(\mathrm{A}t)^{\frac{1}{2}}} \exp(\lambda^2)\, d\lambda \cong 1 - \left[\frac{a \; + \; b\,(At)^{\frac{1}{2}}}{\left(1 - c\,(At)^{\frac{1}{2}} \; + \; d * At\right)(At)^{\frac{1}{2}}} \right] \tag{6}$$

$$P_1 = \frac{nFD^{1/2}C_0}{\pi^{1/2}} \tag{7}$$

$$P_2 = (2\pi)^{3/2} D (MC_0/\rho)^{1/2} N_0 \tag{8}$$

$$P_3 = \left(\frac{2C_0 M}{\pi\rho}\right)^{1/2} z_{WR} F k_{WR} \tag{9}$$

In these equations, λ is the integration variable, n is the electrons number of the palladium electrodeposition reaction, F is the Faraday constant, C_0 and D are the bulk concentration and Pd(II) diffusion coefficient, respectively, M and ρ are the atomic mass and Pd density, respectively, z_{WR} is the number of electrons transferred during the water reduction reaction, k_{WR} is the rate constant of the water reduction reaction on the palladium deposit surface, A is the palladium deposit nucleation frequency, and N_0 is the number density of active sites for palladium nucleation on the electrode surface. The numerical values a = 0.051314213, b = 0.47910725, c = 1.2068142, and d = 1.185724 correspond to the parameters of the polynomial approximation of the Dawson integral.

Therefore, Eqn. (1) can be parameterized as follows:

$$j(t) = (P_3 + P_1 t^{-1/2}) \left(\frac{1 - \left[\frac{a + b\,(At)^{\frac{1}{2}}}{\left(1 - c\,(At)^{\frac{1}{2}} + d * At\right)(At)^{\frac{1}{2}}} \right]}{1 - \frac{1 - exp(-At)}{\mathrm{A}t}} \right) \left(1 - \exp\left(-P_2 t\left(1 - \frac{1 - exp(-At)}{\mathrm{A}t}\right)\right)\right) \tag{10}$$

An example of the application of Eqn. (10) to the analysis of the *j*-*t* plots recorded during the potentiostatic electrodeposition of Pd onto a GCE from ethaline or reline are shown in Fig. 2**(a)** and 2**(b)** respectively.

J. Mex. Chem. Soc. **2025**, *69*(1)
Special Issue

ISSN-e 2594-0317

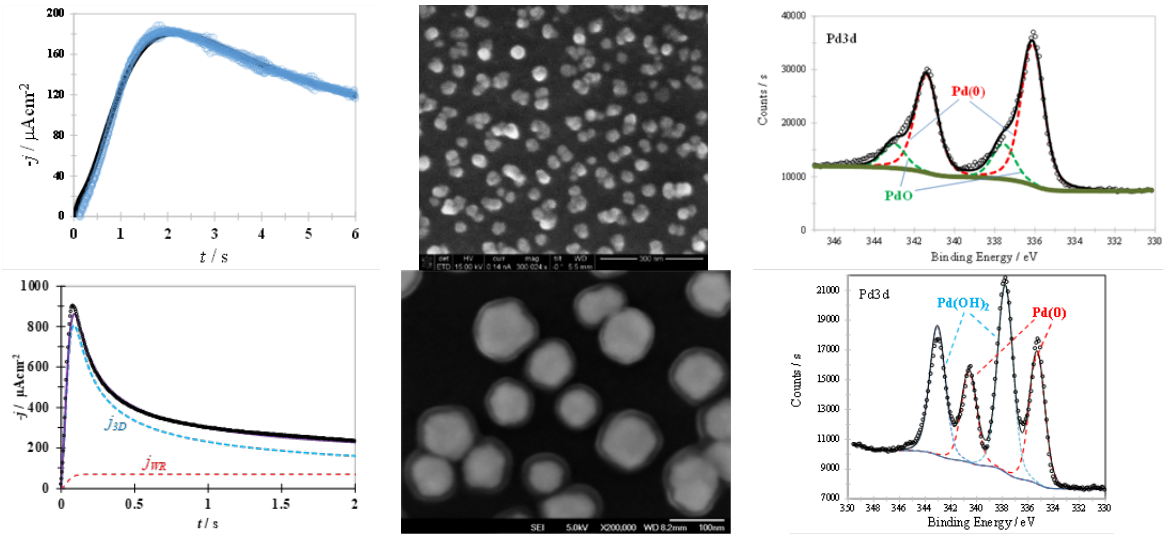

Fig. 2. Comparison of a theoretical potentiostatic current density transient (black solid line) obtained after nonlinear fitting of Eqn. (10) into the experimental data (points) recorded in the system **(a)** GCE / 5 mM $PdCl_2$, dissolved in the eutectic mix of choline chloride and ethylene glycol, ethaline DES, after imposed an overpotential of -0.2 V at 298 K and **(b)** GCE / 5 mM $PdCl_2$, dissolved in the reline eutectic mixture at 343 K for an applied overpotential of –0.40 V, along with its respective SEM and XPS analysis.

Fig. 2**(a)** and 2**(b)** show that the theoretical current density transient fits the experimental data quite well in both cases Furthermore, this formalism indicates that while j_{WR} is absent when ethaline was used at room temperature, it is clearly present during the PdNPs formation from reline. Therefore, based on this analysis, it is expected that PdNPs formed from ethaline would consist of metallic palladium (see R2), while those formed from reline, due to the present of R1, would lead to the formation of core-sell nanoparticles, Pd@$Pd(OH)_2$, through an $E_{R2}E_{R1}C_{R3}$ mechanisms. In this mechanism, the first electrochemical reaction, E_{R2}, corresponds to R2, the second, E_{R1}, to R1 and the chemical reaction, C_{R3}, to R3, which involves the formation of palladium hydroxide, $Pd(OH)_{2(s)}$, by the reaction of Pd(II) ions in reline with OH^- ions formed on the surfaces of $Pd_{(s)}$ nanoparticles. The formation of PdNPs or Pd@$Pd(OH)_2$ are clearly supported by the SEM images and XPS spectra presented in Fig. 2**(a)** and 2**(b)** respectively.

$$\mathrm{Pd(II)_{Reline}} + 2e^- \underset{\leftarrow}{\rightarrow} Pd_{(solid)} \qquad \text{(R2)}$$

$$\mathrm{Pd(II)_{Reline}} + 2OH^- \underset{\leftarrow}{\rightarrow} Pd(OH)_{2(solid)} \qquad \text{(R3)}$$

Conclusions

This review highlights a small fraction of the significant contributions to chemical science made by the UAM community over the past 50 years. Specifically, it focuses on the fundamental and applied aspects of nucleation and growth phenomena in phase formation processes. Although the theoretical models developed for this purpose can be adequately applied to both aqueous and non-aqueous electrolytes (such as deep eutectic solvents, DES), there are still challenges and opportunities for improvement in DES applications in EPF processes. These include the need for more in-depth physical and chemical characterization, such as the speciation of metal ions in this media.

J. Mex. Chem. Soc. **2025**, *69*(1)
Special Issue

ISSN-e 2594-0317

Acknowledgement

I would like to dedicate this work to **Prof. María Teresa Ramírez-Silva** on the occasion of her retirement and recent distinction as an emeritus member of the National System of Researchers (SNII) of CONACHYT. I am deeply indebted to all my professors, colleagues, and students; without their support, this work would not have been possible and SNI for the distinction of its membership.

References

1. Palomar-Pardavé, M.; Ramírez, M. T.; González, I.; Serruya, A.; Scharifker, B. R. *J. Electrochem. Soc.* **1996**, *143*, 1551–1558. DOI: http://dx.doi.org/10.1149/1.1836678.
2. Serruya, A.; Scharifker, B. R.; González, I.; Oropeza, M. T.; Palomar-Pardavé, M. *J. Appl. Electrochem.* **1996**, *26*, 451–457. DOI: https://doi.org/10.1007/BF00251332.
3. Scharifker, B. R.; Mostany, J.; Palomar-Pardavé, M.; González, I. *J. Electrochem. Soc.* **1999**, *146*, 1005–1012. DOI: http://dx.doi.org/10.1149/1.1391713.
4. Palomar-Pardavé, M.; González, I.; Batina, N. *J. Phys. Chem. B.* **2000**, *104*, 3545–3555. DOI: https://doi.org/10.1021/jp9931861.
5. Barrera, E.; Palomar-Pardavé, M.; Batina, N.; González, I. *J. Electrochem. Soc.* **2000**, *147*, 1787–1796. DOI: https://doi.org/10.1149/1.1393435.
6. Mendoza-Huizar, L. H.; Robles, J.; Palomar-Pardavé, M. *J. Electroanal. Chem.* **2002**, *521*, 95-106. DOI: https://doi.org/10.1016/S0022-0728(02)00659-9.
7. Espinoza-Ramos, L. I.; Hallen-López, J. M.; Ramírez, C.; Arce, E.; Palomar-Pardavé, M.; Romero-Romo, M. *J. Electrochem. Soc.* **2002**, *149*, B543–B550. DOI: https://doi.org/10.1149/1.1517580.
8. Mendoza-Huizar, L. H.; Robles, J.; Palomar-Pardavé, M. *J. Electroanal. Chem.* **2003**, *545*, 39-45. DOI: https://doi.org/10.1016/S0022-0728(03)00087-1.
9. Martínez-Ruíz, A.; Palomar-Pardavé, M.; Valenzuela-Benavides, J.; Farías, M.; Batina, N. *J. Phys. Chem. B.* **2003**, *107*, 11660–11665. DOI: https://doi.org/10.1021/jp027197x.
10. Ramírez, C.; Arce, E. M.; Romero-Romo, M.; Palomar-Pardavé, M. *Solid State Ion.* **2004**, *169*, 81–85. DOI: http://dx.doi.org/10.1016/j.ssi.2004.01.023.
11. Sánchez-Rivera, A. E.; Vital-Vaquier, V.; Romero-Romo, M.; Palomar-Pardavé, M.; Ramírez-Silva, M. T. *J. Electrochem. Soc.* **2004**, *151*, C666–C673. DOI: https://doi.org/10.1149/1.1789373.
12. Palomar-Pardavé, M.; Scharifker, B. R.; Arce, E. M.; Romero-Romo, M. *Electrochim. Acta.* **2005**, *50*, 4736–4745. DOI: https://doi.org/10.1016/j.electacta.2005.03.004.
13. Cobos-Murcia, A.; Galicia, L.; Rojas-Hernández, A.; Ramírez-Silva, M. T.; Álvarez- Bustamante, R.; Romero-Romo, M.; Rosquete-Pina, G.; Palomar-Pardavé, M. *Polymer.* **2005**, *46*, 9053–9063. DOI: https://doi.org/10.1016/j.polymer.2005.07.026.
14. Álvarez-Romero, G. A.; Garfias-García, E.; Ramírez-Silva, M. T.; Galán-Vidal, C.; Romero-Romo, M.; Palomar-Pardavé, M. *Appl. Surface Sci.* **2006**, *252*, 5783–5792. DOI: https://doi.org/10.1016/j.apsusc.2005.07.060.
15. Álvarez-Romero, G. A.; Palomar-Pardavé, M. E.; Ramírez-Silva, M. T. *Anal. Bioanal. Chem.* **2007**, *387*, 1533-1541. DOI: https://doi.org/10.1007/s00216-006-1021-1.
16. Corona-Avendaño, S.; Alarcón-Angeles, G.; Ramírez-Silva, M. T.; Rosquete-Pina, G.; Romero-Romo, M.; Palomar-Pardavé, M. *J. Electroanal. Chem.* **2007**, *609*, 17-26. DOI: https://doi.org/10.1016/j.jelechem.2007.05.021.
17. Garfias-García, E.; Romero-Romo, M.; Ramírez-Silva, M. T.; Morales, J.; Palomar- Pardavé, M. *J. Electroanal. Chem.* **2008**, *613*, 67–79. DOI: https://doi.org/10.1016/j.jelechem.2007.10.013.
18. Martínez-Ruiz, A.; Palomar-Pardavé, M.; Batina, N. *Electrochim. Acta.* **2008**, *53*, 2115-2120. DOI: https://doi.org/10.1016/j.electacta.2007.09.011.

J. Mex. Chem. Soc. **2025**, *69*(1)
Special Issue

ISSN-e 2594-0317

19. Alarcón-Angeles, G.; Corona-Avendaño, S.; Ramírez-Silva, M. T.; Rojas-Hernández, A.; Romero-Romo, M.; Palomar-Pardavé, M. *Electrochim. Acta.* **2008**, *53*, 3013-3020. DOI: http://dx.doi.org/10.1016/j.electacta.2007.11.016.
20. Corona-Avendaño, S.; Alarcón-Angeles, G.; Ramírez-Silva, M. T.; Romero-Romo, M.; Cuán, A.; Palomar-Pardavé, M. *J. Electrochem. Soc.* **2009**, *156*, J375-J381. DOI: https://doi.org/10.1149/1.3223664.
21. Aguilar-Sánchez, M.; Palomar-Pardavé, M.; Romero-Romo, M.; Ramírez-Silva, M. T.; Barrera, E.; Scharifker, B. R. *J. Electroanal. Chem.* **2010**, *647*, 128-132. DOI: http://dx.doi.org/10.1016/j.jelechem.2010.06.012.
22. Licona-Sánchez, T. J.; Álvarez-Romero, G. A.; Mendoza-Huizar, L. H.; Galán- Vidal, C. A.; Palomar-Pardavé, M.; Romero-Romo, M.; Herrera-Hernández, H.; Uruchurtu, J.; Juárez-García, J. M. *J. Phys. Chem. B.* **2010**, *114*, 9737–9743. DOI: https://doi.org/10.1021/jp102676q.
23. Corona-Avendaño, S.; Ramírez-Silva, M. T.; Palomar-Pardavé, M.: Hernández-Martínez, L.: Romero-Romo, M.: Alarcón-Ángeles, G. *J. Appl. Electrochem.* **2010**, *40*, 463-474. DOI: http://dx.doi.org/10.1007/s10800-009-0017-x.
24. Garfias-García, E.; Romero-Romo, M.; Ramírez-Silva, M. T.; Morales, J.; Palomar-Pardavé, M. *Int. J. Electrochem. Sci.* **2010**, *5*, 763-773. DOI: https://doi.org/10.1016/S1452-3981(23)15321-1.
25. Alarcón-Ángeles, G.; Guix, M.; Silva, W. C.; Ramírez-Silva, M. T.; Palomar-Pardavé, M.; Romero-Romo, M.; Merkoci, A. *Biosens. Bioelectron.* **2010**, *26*, 1768–1773. DOI: https://doi.org/10.1016/j.bios.2010.08.058.
26. Hernández-Espejel, A.; Palomar-Pardavé, M.; Cabrera-Sierra, R.; Romero-Romo, M.; Ramírez-Silva, M. T.; Arce-Estrada, E. M. *J. Phys. Chem. B.* **2011**, *115*, 1833–1841. DOI: https://doi.org/10.1021/jp106851b.
27. Licona-Sánchez, T. J.; Álvarez-Romero, G. A.; Palomar-Pardavé, M.; Galán-Vidal, C. A.; Páez-Hernández, M. E.; Ramírez-Silva, M. T.; Romero-Romo, M. *Int. J. Electrochem. Sci.* **2011**, *6*, 1537 – 1549. DOI: https://doi.org/10.1016/S1452-3981(23)15091-7.
28. Palomar-Pardavé, M.; Garfias-García, E.; Romero-Romo, M.; Ramírez-Silva, M. T.; Batina, N. *Electrochim. Acta.* **2011**, *56*, 10083-10092. DOI: https://doi.org/10.1016/j.electacta.2011.08.105.
29. Rodríguez- Bravo, L. A.; Palomar- Pardavé, M.; Corona-Avendaño, S.; Romero-Romo, M.; Herrera-Hernández, H.; Ramírez-Silva, M. T.; Escarela-Pérez, R. *Int. J. Electrochem. Sci.* **2011**, *6*, 2730 – 2745. DOI: https://doi.org/10.1016/S1452-3981(23)18213-7.
30. Garfias-García, E.; Romero-Romo, M.; Ramírez-Silva, M. T.; Palomar- Pardavé, M. I*nt. J. Electrochem. Sci.* **2012**, *7*, 3102-3114. DOI: https://doi.org/10.1016/S1452-3981(23)13938-1.
31. Colín-Orozco, E.; Ramírez-Silva, M. T.; Corona-Avendaño, S.; Romero-Romo, M.; Palomar-Pardavé, M. *Electrochim. Acta.* **2012**, *85*, 307–313. DOI: https://doi.org/10.1016/j.electacta.2012.08.081.
32. Palomar-Pardavé, M.; Ramírez-Silva, M. T.; Vázquez-Coutiño, G. A.; Romero-Romo, M.; Herrera-Hernández, H.; Montes de Oca-Yemha, M. G. J. *Solid State Electrochem.* **2013**, *17*, 459. DOI: http://dx.doi.org/10.1007/s10008-012-1882-5.
33. Corona-Avendaño, S.; Ramírez-Silva, M. T.; Romero-Romo, M.; Rojas-Hernández, A.; Palomar-Pardavé, M. *Electrochim. Acta.* **2013**, *89*, 854–860. DOI: https://doi.org/10.1016/j.electacta.2012.10.165.
34. Guzmán-Hernández, D. S.; Palomar-Pardavé, M.; Rojas-Hernández, A.; Corona-Avendaño, S.; Romero-Romo, M.; Ramírez-Silva, M. T. *Electrochim. Acta.* **2014**, *140*, 535–540. DOI: https://doi.org/10.1016/j.electacta.2014.05.092.
35. Ramírez-Silva, M. T.; Palomar-Pardavé, M.; Corona-Avendaño, S.; Romero-Romo, M.; Alarcón-Angeles, G. *Molecules.* **2014**, *19*, 5952-5964. DOI: http://dx.doi.org/10.3390/molecules19055952.
36. Palomar-Pardavé, M.; Corona-Avendaño, S.; Romero-Romo, M.; Alarcón-Angeles, G.; Merkoçi, A.; Ramírez-Silva, M. T. *J. Electroanal. Chem.* **2014**, *717-718*, 103–109. DOI: https://doi.org/10.1016/j.jelechem.2014.01.002.

J. Mex. Chem. Soc. **2025**, *69*(1)
Special Issue

ISSN-e 2594-0317

37. Aldana-González, J.; Olvera-García, J.; Montes de Oca, M. G.; Romero-Romo, M.; Ramírez-Silva, M. T.; Palomar-Pardavé, M. *Electrochem. Commun.* **2015**, *56*, 70–74. DOI: https://doi.org/10.1016/j.elecom.2015.04.014.
38. Branco P. D.; Saavedra, K.; Palomar-Pardavé, M.; Borrás, C.; Mostany, J.; Scharifker, B. R. *J. Electroanal. Chem.* **2016**, *765*, 140–148. DOI: https://doi.org/10.1016/j.jelechem.2015.10.011.
39. Palomar-Pardavé, M.; Aldana-González, J.; Botello, L. E.; Arce-Estrada, E. M.; Ramírez-Silva, M. T.; Mostany, J.; Romero-Romo, M. *Electrochim. Acta.* **2017**, *241*, 162–169. DOI: https://doi.org/10.1016/j.electacta.2017.04.126.
40. Aldana-González, J.; Uruchurtu-Chavarin, J.; Montes de Oca, M. G.; Ramírez-Silva, M. T.; Palomar-Pardavé, M.; Romero-Romo, M. *Int. J. Electrochem. Sci.* **2016**, *11*, 9402–9412. DOI: https://doi.org/10.20964/2016.11.54.
41. Sebastián, P.; Botello, L. E.; Vallés, E.; Gómez, E.; Palomar-Pardavé, M.; Scharifker, B. R.; Mostany, J. *J. Electroanal. Chem.* **2017**, *793*, 119-125. DOI: https://doi.org/10.1016/j.jelechem.2016.12.014.
42. Romero-Romo, M.; Aldana-González, J.; Botello, L. E.; Montes de Oca, M. G.; Ramírez-Silva, M. T.; Corona-Avendaño, S.; Palomar-Pardavé, M. *J. Electroanal. Chem.* **2017**, *791*, 1–7. DOI: https://doi.org/10.1016/j.jelechem.2017.03.003.
43. Manh, T. L.; Arce-Estrada, E. M.; Romero-Romo, M.; Mejía-Caballero, I.; Aldana-González, J.; Palomar-Pardavé, M. *J. Electrochem. Soc.* **2017**, *164*, D694-D699. DOI: http://dx.doi.org/10.1149/2.1061712jes.
44. Aldana-González, J.; Romero-Romo, M.; Robles-Peralta, J.; Morales-Gil, P.; Palacios-González, E.; Ramírez-Silva, M. T.; Mostany, J.; Palomar-Pardavé, M. *Electrochim. Acta*. **2018**, *276*, 417–423. DOI: https://doi.org/10.1016/j.electacta.2018.04.192.
45. Manh, T.L.; Arce-Estrada, E. M.; Mejía-Caballero, I.; Aldana-González, J.; Romero- Romo, M.; Palomar-Pardavé, M. *J. Electrochem. Soc.* **2018**, *165*, D285-D290. DOI: http://dx.doi.org/10.1149/2.0941807jes.
46. Manh, T.L.; Arce-Estrada, E. M.; Mejía-Caballero, I.; Rodríguez-Clemente, E.; Sánchez, W.; Aldana-Gonzále, J.; Lartundo-Rojas, L.; Romero-Romo, M.; Palomar-Pardavé, M. *J. Electrochem. Soc.* **2018**, 165, D808-D812. DOI: https://doi.org/10.1149/2.0561816jes.
47. Espino-López, I. E.; Romero-Romo, M.; Montes de Oca-Yemha, M. G.; Morales-Gil, P.; Ramírez-Silva, M. T.; Mostany, J.; Palomar-Pardavé, M. *J. Electrochem. Soc.* **2019**, *166*, D3205-D3211. DOI: https://doi.org/10.1149/2.0251901jes.
48. Rodríguez-Clemente, E.; Manh, T.L.; Guinto-Pano, C. E.; Romero-Romo, M.; Mejía-Caballero, I.; Morales-Gil, P.; Palacios-González. E.; Palomar-Pardavé, M. *J. Electrochem. Soc.* **2019**, *166*, D3035-D3041. DOI: https://doi.org/10.1149/2.0051901jes.
49. Aldana-González, J.; Sampayo-Garrido, A.; Montes de Oca-Yemha, M. G.; Sánchez, W.; Ramírez-Silva, M. T.; Arce-Estrada, E. M.; Romero-Romo, M.; Palomar-Pardavé, M. *J. Electrochem. Soc.* **2019**, *166*, D199-D204. DOI: https://doi.org/10.1149/2.0761906jes.
50. Palomar-Pardavé, M.; Mostany, J.; Muñoz-Rizo, R.; Botello, L. E.; Aldana-González, J.; Arce-Estrada, E. M.; Montes de Oca-Yemha, M. G.; Ramírez-Silva, M. T.; Romero-Romo, M. *J. Electroanal. Chem.* **2019**, *851*, 113453. DOI: http://dx.doi.org/10.1016/j.jelechem.2019.113453.
51. Juárez-Marmolejo, L.; Maldonado-Teodocio, B.; Montes de Oca-Yemha, M. G.; Romero-Romo, M.; Ramírez-Silva, M. T.; Arce-Estrada, E. M.; Morales-Gil, P.; Mostany, J.; Palomar-Pardavé, M. *J. Phys. Chem. B.* **2020**, *124*, 3973-3983. DOI: https://doi.org/10.1021/acs.jpcb.0c01014.
52. Landa-Castro, M.; Aldana-González, J.; Montes de Oca-Yemha, M. G.; Romero-Romo, M.; Arce-Estrada, E. M.; Palomar-Pardavé, M. *J. Alloys Compd.* **2020**, *830*, 154650. DOI: https://doi.org/10.1016/j.jallcom.2020.154650.
53. Juárez-Marmolejo, L.; Maldonado-Teodocio, B.; Montes de Oca-Yemha, M. G.; Romero-Romo, M.; Ramírez-Silva, M. T.; Arce-Estrada, E. M.; Morales-Gil, P.; Mostany, J.; Palomar-Pardavé, M. *J. Electrochem. Soc.* **2020**, *167*, 112509. DOI: http://dx.doi.org/10.1149/1945-7111/aba7d9.

J. Mex. Chem. Soc. **2025**, *69*(1)
Special Issue

ISSN-e 2594-0317

54. Sánchez-Ortiz, W.; Aldana-González, J.; Manh, T. L.; Romero-Romo, M.; Mejía-Caballero, I.; Ramírez-Silva, M. T.; Arce-Estrada, E. M.; Mugica-Álvarez, V.; Palomar-Pardavé, M. *J. Electrochem. Soc.* **2021**, *168*, 016508. DOI: https://doi.org/10.1149/1945-7111/abdb01.
55. Mejía-Caballero, I.; Manh, T. L.; Aldana-González, J.; Arce-Estrada, E. M.; Romero-Romo, M.; Campos-Silva, I.; Ramírez-Silva, M. T.; Palomar-Pardavé, M. *J. Electrochem. Soc.* **2021**,*168*, 112512. DOI: https://doi.org/10.1149/1945-7111/ac39d7.
56. Juárez-Marmolejo, L.; Maldonado-Teodocio, B.; Montes de Oca-Yemha, M. G.; Romero-Romo, M.; Arce-Estrada, E. M.; Ezeta-Mejía, A.; Ramírez-Silva, M. T.; J. Mostany, J.; Palomar-Pardavé, M. *Catal. Today*. **2022**, *394-396*, 190-197. DOI: https://doi.org/10.1016/j.cattod.2021.10.012.
57. Vidal-García, G.; Guinto-Pano, C. E.; García-Hernández, I.; Rodríguez-Clemente, E.; Morales-Gil, P.; Ramírez-Silva, M. T.; Romero-Romo, M.; Palomar-Pardavé, M. T. *Nonferr. Metal. Soc. China.* **2022**, *32*, 1050−1060. DOI: https://doi.org/10.1016/S1003-6326(22)65854-0.
58. Martínez-Guerra, J.; Palomar-Pardavé, M.; Romero-Romo, M.; Corona-Avendaño, S.; Guzmán-Hernández, D. S.; Rojas-Hernández, A.; Ramírez-Silva, M. T. *ChemElectroChem.* **2022**, *9*, e202101534. DOI: https://doi.org/10.1002/celc.202101534.
59. Aldana-González, J.; Sampayo-Garrido, A.; Hernández-Pérez, D.; Montes de Oca-Yemha, M. G.; Arce-Estrada, E. M.; Ramírez-Silva, M. T.; Morales-Gil, P.; Romero-Romo, M.; Mugica-Álvarez, V.; Palomar-Pardavé, M. *J. Electrochem. Soc.* **2022**, *169*, 102504. DOI: https://doi.org/10.1149/1945-7111/ac96b3.
60. Landa-Castro, M.; Romero-Romo, M.; Arce-Estrada, E. M.; Morales-Gil, P.; Montes de Oca-Yemha, M. G.; Palomar-Pardavé, M. *J. Electrochem. Soc.* **2022**, *169*, 092521. DOI: https://doi.org/10.1149/1945-7111/ac91fa.
61. Godoy-Colin, E.; Corona-Avendaño, S.; Ramírez-Silva, M. T.; Aldana-Gonzalez, J.; Vázquez-Huerta, G.; Ángeles-Beltrán, D.; Romero-Romo, M.; Palomar-Pardavé, M. *J. Electrochem. Soc.* **2022**, *169*, 092506. DOI: http://dx.doi.org/10.1149/1945-7111/ac8d31.
62. Thuy-Linh Phi; Son Tang Nguyen; Nguyen Van Hieu; Palomar-Pardavé, M.; Morales-Gil, P.; Manh, T. L. *Inorg. Chem.* **2022**, *61*, 5099−5111. DOI: https://doi.org/10.1021/acs.inorgchem.2c00127.
63. Morales-Gil, P.; Montes de Oca-Yemha, M. G.; Pérez-Cruz, F.; Romero-Romo, M.; Ramírez-Silva, M. T.; Aldana-González, J.; Palomar Pardavé, M. *J. Mol. Liq.* **2023**, *386*, 122499. DOI: https://doi.org/10.1016/j.molliq.2023.122499.
64. Hernández-Perez, D.; Aldana-González, J.; Sánchez-Ortiz, W.; Romero-Romo, M.; Arce-Estrada, E. M.; Palomar-Pardavé, M. *J. Solid State Electr.* **2023**, *27*, 3067-3073. DOI: http://dx.doi.org/10.1007/s10008-023-05568-w.
65. Vidal-García, G.; Aldana-González, J.; Romero-Romo, M.; Ramírez-Silva, M. T.; Teutli-León, M. M. M.; Hernández-Pérez, D.; Mostany, J.; Scharifker, B. R.; Palomar-Pardavé, M. *J. Solid State Electr.* **2024**, *28*, 1631–1639. DOI: http://dx.doi.org/10.1007/s10008-023-05623-6.
66. Basilio-Brito, A.; Landa-Castro, M.; Sánchez-Ortiz, W.; Rivera-Hernández, S.; Romero-Romo, M.; Arce-Estrada, E. M.; Aldana-González, J.; Palomar-Pardavé, M. *Electrocatalysis.* **2023**, *14*, 868-874. http://dx.doi.org/10.1007/s12678-023-00842-x.
67. Hoang Thi Thanh Thuy; Nang Xuan Ho; Vinh Nguyen Duy; Thuy Cao Thi; Tuan Pham Anh; Morales-Gil, P.; Palomar-Pardavé, M.; Nguyen Van Hieu; Thi-Xuan Chu; Manh, T. L. *J. Solid State Electr.* **2024**, *28*, 255-271. DOI: http://dx.doi.org/10.21203/rs.3.rs-2539558/v1.
68. Mejía-Caballero, I.; Aldana-González, J.; Manh, T. L.; Romero-Romo, M.; Arce- Estrada, E. M.; Campos-Silva, I.; Ramírez-Silva, M. T.; Palomar-Pardavé, M. *J. Electrochem. Soc.* **2018**, *165*, D393-D401. DOI: https://doi.org/10.1149/2.0851809jes.
69. Quiroz, M. A.; Gonzalez, I.; Meas, Y.; Lamy-Pitara, E.; Barbier, J. *Electrochim. Acta.* **1987**, *32*, 289-291. DOI: https://doi.org/10.1016/0013-4686(87)85037-5.
70. Trejo, G.; Gil, A. F.; González, I. *J. Electrochem. Soc.* **1995**, *142*, 3404-3408. DOI: https://doi.org/10.1149/1.2049994.

J. Mex. Chem. Soc. **2025**, *69*(1)
Special Issue

ISSN-e 2594-0317

71. Trejo, G.; Gil, A. F.; González, I. *J. Appl. Electrochem.* **1996**, *26*, 1287-1294. DOI: https://link.springer.com/content/pdf/10.1007/BF00249932.pdf.
72. Nila, C.; González, I. *J. Electroanal. Chem.* **1996**, *1*, 171-182. DOI: https://doi.org/10.1016/0022-0728(95)04278-4.
73. Miranda-Hernández, M.; González, I. *Electrochim. Acta.* **1997**, *42*, 2295-2303. DOI: https://doi.org/10.1016/S0013-4686(96)00394-5.
74. Ramos, A.; Miranda-Hernández, M.; González, I. *J. Electrochem. Soc.* **2001**, *148*, C315-C321. DOI: https://doi.org/10.1149/1.1357176.
75. Miranda-Hernández, M.; González, I.; Batina, N. *J. Phys. Chem. B.* **2001**, *105*, 4214-4223. DOI: https://doi.org/10.1021/jp002057d.
76. Poisot-Díaz, M. E.; González, I.; Lapidus, G. T. *Hydrometallurgy.* **2008**, *93*, 23-29. DOI: https://doi.org/10.1016/j.hydromet.2008.02.015.
77. Carrera-Crespo, J. E.; Acevedo-Peña, P.; Miranda-Hernández, M.; González, I. *J. Solid State Electr.* **2013**, *17*, 445-457. DOI: http://dx.doi.org/10.1007/s10008-012-1975-1.
78. Landa, M.; Sebastian Pascual, P.; Giannotti, M. I.; Serrà, A.; Gómez, E. *Electrochim. Acta.* **2020**, 359, 136928. DOI: http://dx.doi.org/10.1016/j.electacta.2020.136928.
79. Serrà, A.; Sebastian Pascual, P.; Landa, M.; Gómez, E. *J. Electroanal. Chem.* **2021**, *896*, 115177. DOI: https://doi.org/10.1016/j.jelechem.2021.115177.
80. Heerman, L.; Tarallo, A. *Electrochem. Commun.* **2000**, *2*, 85-89. DOI: http://dx.doi.org/10.1016/S1388-2481(99)00144-7.
81. Milchev, A.; Montenegro, M. I. *J. Electroanal. Chem.* **1992**, *333*, 93-102. DOI: https://doi.org/10.1016/0022-0728(92)80383-F.
82. Palomar-Pardavé, M. E.; Le, T. in: *Manh Editors. Nucleation and Growth in Applied Materials*. Elsevier Radarweg 29, PO Box 211, 1000 AE Amsterdam, Netherlands 125 London Wall, London EC2Y 5AS, United Kingdom 50 Hampshire Street, 5th Floor, Cambridge, MA 02139, United States. 2024, ISBN: 978-0-323-99537-5. DOI: https://doi.org/10.1016/C2021-0-02052-6.
83. Milchev, A. in: *Electrocrystallisation, Fundamentals of Nucleation and Growth*, Kluwer, New York, 2002.
84. Philipp, R.; Retter, U. *Electrochim. Acta.* 1995, *40*, 1581-1585. DOI: https://doi.org/10.1016/0013-4686(95)00100-S.
85. Gunawardena, G. A.; Hills, G. J.; Montenegro, I.; Scharifker, B. R. *J. Electroanal. Chem.* **1982**, *138*, 225. DOI: https://doi.org/10.1016/0022-0728(82)85080-8.
86. Scharifker, B. R.; Mostany, J. *J. Electroanal. Chem.* **1984**, *177*, 13–23. DOI: https://doi.org/10.1016/0022-0728(84)80207-7.